

See discussions, stats, and author profiles for this publication at: <https://www.researchgate.net/publication/265213820>

Anion Radicals of Isomeric [5,6] and [6,6] Benzoadducts of Sc₃N@C-80: Remarkable Differences in Endohedral Cluster Spin Density and Dynamics

ARTICLE *in* JOURNAL OF THE AMERICAN CHEMICAL SOCIETY · AUGUST 2014

Impact Factor: 12.11 · DOI: 10.1021/ja507607k · Source: PubMed

CITATIONS

2

READS

72

5 AUTHORS, INCLUDING:



Alexey A Popov

Leibniz Institute for Solid State and Materials ...

188 PUBLICATIONS 3,417 CITATIONS

[SEE PROFILE](#)



Anastasia Pykhova

Lomonosov Moscow State University

2 PUBLICATIONS 10 CITATIONS

[SEE PROFILE](#)



Fang-Fang Li

University of Texas at El Paso

17 PUBLICATIONS 422 CITATIONS

[SEE PROFILE](#)



Luis Echegoyen

University of Texas at El Paso

445 PUBLICATIONS 13,337 CITATIONS

[SEE PROFILE](#)

Anion Radicals of Isomeric [5,6] and [6,6] Benzoadducts of $\text{Sc}_3\text{N}@\text{C}_{80}$: Remarkable Differences in Endohedral Cluster Spin Density and Dynamics

Alexey A. Popov,*[†] Anastasia D. Pykhova,[‡] Ilya N. Ioffe,[‡] Fang-Fang Li,^{§,||} and Luis Echegoyen*,[§]

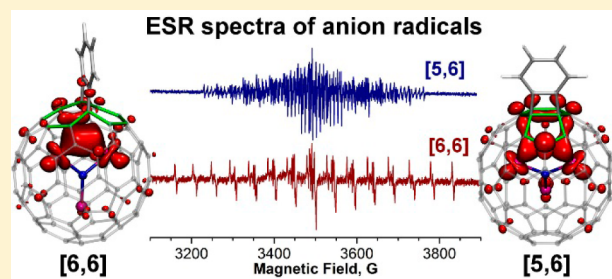
[†]Leibniz Institute for Solid State and Materials Research, 01069 Dresden, Germany

[‡]Chemistry Department, Moscow State University, 119992 Moscow, Russian Federation

[§]Department of Chemistry, University of Texas at El Paso, El Paso, Texas 79968, United States

Supporting Information

ABSTRACT: The anion radicals of isomeric [5,6] and [6,6] $\text{Sc}_3\text{N}@\text{C}_{80}$ benzoadducts were studied by electron spin resonance spectroscopy, density functional theory computations, and molecular dynamics. In both compounds the rotation of the Sc_3N cluster is frozen and the spin density distribution of the cluster is highly anisotropic, with hyperfine coupling constants of 9.1 and 2×33.3 G for the [5,6] adduct and ~ 0.6 and 2×47.9 G for the [6,6] adduct. Remarkably, the subtle variation of the position of the exohedral group on the surface of the cage results in very pronounced changes in the spin density distribution and the dynamics of the encapsulated Sc_3N cluster.



INTRODUCTION

Encapsulation of a metal cluster inside a carbon cage results in very unique electronic properties of endohedral metallofullerenes (EMFs).^{1–5} Endohedral monometallofullerenes typically exhibit cage-based redox activity. EMFs encapsulating more complex endohedral species, such as dimetallocfullerenes or some clusterfullerenes, can exhibit either fullerene-based or endohedral-group redox activity, depending on the match of the cluster and carbon cage frontier molecular orbitals (MOs).^{6,7} In particular, the LUMO of the archetypical nitride clusterfullerene $\text{Sc}_3\text{N}@\text{C}_{80}$ is largely localized on the Sc_3N cluster,^{8–10} which leads to cluster-based electrochemical reduction and a correspondingly large electron spin resonance (ESR) ^{45}Sc hyperfine coupling (hfc) constant of ca. 56 G for the anion radical.^{11,12} Both computational and experimental studies have shown that in the highly isotropic environment of the icosahedral I_h -symmetric carbon cage, the Sc_3N cluster rotates almost freely on the nanosecond time scale.^{8,13–15}

The extended π systems of fullerenes are subject to exohedral modifications via cycloadditions or radical additions (CF_3). Under the assumption that the cluster rotates freely and rapidly, $\text{Sc}_3\text{N}@\text{C}_{80}\text{-}I_h$ exhibits only two types of C–C bonds, denoted as [5,6] and [6,6], i.e. pentagon/hexagon and hexagon/hexagon edges, respectively. Although [5,6] cycloadducts are usually thermodynamically preferred,^{16–21} benzyne addition to $\text{Sc}_3\text{N}@\text{C}_{80}$ affords both [5,6] and [6,6] monocycloadducts (Figure 1).²² Chemical functionalization of the carbon cage typically changes the fullerene π system (since some sp^2 -hybridized carbon atoms change their hybridization state to sp^3) and thus affects the frontier MO energies. Electrochemical studies of the

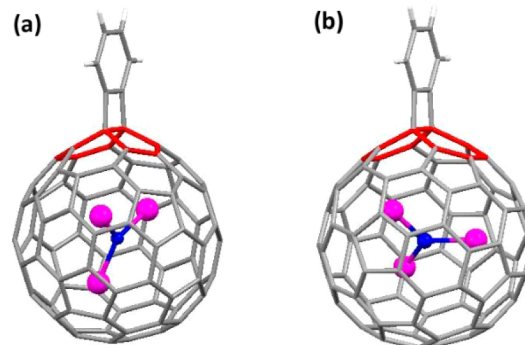


Figure 1. Molecular structures of (a) [5,6] and (b) [6,6] benzcycloadducts of $\text{Sc}_3\text{N}@\text{C}_{80}$. The [5,6] and [6,6] rings involved in the additions are highlighted in red.

[5,6] and [6,6] benzcycloadducts of $\text{Sc}_3\text{N}@\text{C}_{80}$ showed that both addition modes stabilize the LUMO and shift the first reduction potential from -1.26 V [vs the $\text{Fe}(\text{Cp})_2^{+/\text{0}}$ redox couple] for pristine $\text{Sc}_3\text{N}@\text{C}_{80}$ to -1.11 V for the [5,6] adduct and -1.08 V for the [6,6] adduct.

The decrease in the symmetry of the π system in the cycloadducts (C_s instead of I_h) also makes the endohedral environment less isotropic than in the pristine $\text{Sc}_3\text{N}@\text{C}_{80}$ molecule. Therefore, even small modifications of the π system can dramatically affect the dynamics and electronic properties

Received: July 25, 2014

of the endohedral cluster.^{9,19,23–26} Whereas the energetic characteristics of such modifications are accessible via electrochemical studies, experimental access to the LUMO contributions and cluster dynamics are less straightforward. In this work, we utilized the high sensitivity of the ⁴⁵Sc hyperfine structure of the ESR spectra of the anion radicals to analyze the spin density distributions and to study the influence of the isomeric cycloaddition on the LUMO composition and the Sc₃N cluster dynamics.

■ EXPERIMENTAL AND COMPUTATIONAL DETAILS

ESR spectra were measured at room temperature using an X-band EPR spectrometer (EMX Bruker, Germany). The spectra were simulated using the EasySpin suite.²⁷

Density functional theory (DFT) computations were carried out within the generalized gradient approximation (GGA) with the PBE functional²⁸ for the exchange–correlation term, as implemented in the PRIRODA package.^{29–31} All of the conformers were first optimized using an original TZ2P-quality basis set [full-electron {6,3,2}/(11s,6p,2d) for C and N and an SBK-type effective core potential for Sc atoms with a {5,5,4}/(9s,9p,8d) valence part]. The lowest-energy conformers were then reoptimized using the Λ2m basis {4,3,2,1}/(12s,8p,4d,2f) for carbon atoms and the Λ33 basis for nitrogen {8,7,5,3,1}/(14s,10p,7d,5f,3g) and Sc {10,9,7,5,3,1}/(27s,22p,16d,10f,8g,4h).³⁰ Relative energies discussed in the text were obtained at the PBE/(Λ2m, Λ33) level.

Computations of hfc constants with the ORCA package^{32,33} were performed with two combinations of basis sets. One comprised a TZVP {5,3,1}/(11s,6p,1d) basis set³⁴ for carbon atoms and def2-TZVP basis sets³⁵ for N {5,3,2}/(11s,6p,2d) and Sc {6,5,4,2}/(17s12p7d2f) (f and g polarization functions were removed from the original def2-TZVP basis sets for N and Sc, respectively). For computations of hfc constants along MD trajectories, we used the SVP basis for carbon, the TZVP basis for nitrogen, and the core-property CP3P {17,6,3}/(17s,10p,5d) basis³⁶ for Sc.

Born–Oppenheimer molecular dynamics calculations were performed using the CP2K code^{37,38} and employed the velocity Verlet algorithm with a time step of 0.5 fs and a Nosé–Hoover thermostat set at 300 K. Before production runs, the systems were first thermostated for 5 ps. Calculations were performed with the PBE functional and employed Gaussian and plane-wave GPW schemes with Goedecker–Teter–Hutter pseudopotentials and the DZVP basis set.^{37,39,40}

Molecular structures were visualized using the VMD package.⁴¹

■ RESULTS AND DISCUSSION

ESR Spectra of Anion Radicals. The [5,6] and [6,6] benzoadducts were synthesized as described in ref 22. The adducts exhibit reversible reduction behavior showing that their anion radicals are fairly stable at room temperature in *o*-dichlorobenzene (*o*-DCB) solution.²² In this work, the anion radicals of Sc₃N@C₈₀ benzoadducts in *o*-DCB solutions were obtained by addition of approximately equimolar amounts of cobaltocene, Co(Cp)₂. The oxidation potential of Co(Cp)₂ is near −1.3 V,⁴² which is more negative than the first reduction potentials of both benzoadducts, close to their second reduction potentials, and much more positive than their third reduction potentials near −2.2 V.²² Thus, Co(Cp)₂ was a very convenient reducing agent for the present ESR study since there was no risk of the formation of the trianion radical in the case of excess reducing agent. Besides, the ESR signal of Co(Cp)₂ is very broad at room temperature and did not interfere with the measurement, whereas the cation is diamagnetic and hence has no signal at all. Therefore, monoanion radicals of Sc₃N@C₈₀ benzoadducts were the only ESR-active species that could be produced in the mixture of the Sc₃N@C₈₀ benzoadducts with Co(Cp)₂ (formation of

the diamagnetic dianion in the case of excess reducing agent would not produce an ESR signal either). Figure 2 shows the

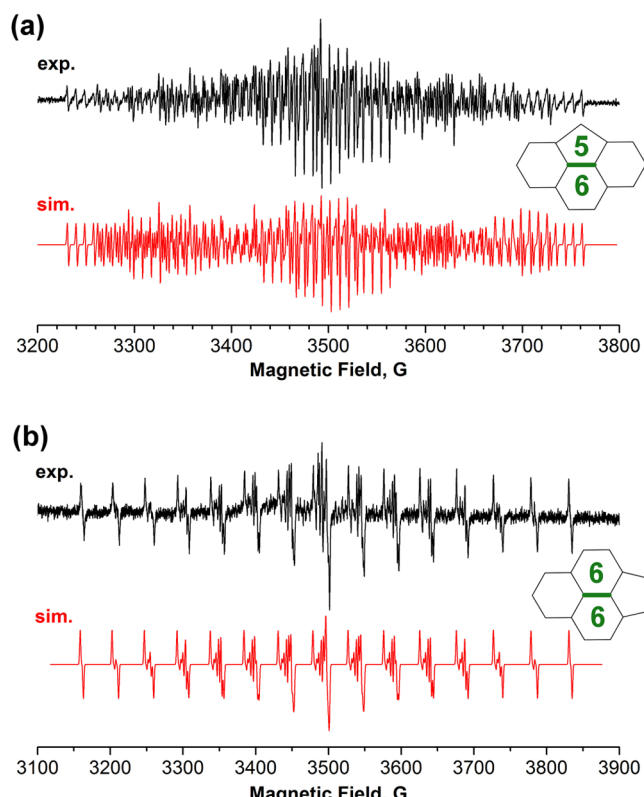


Figure 2. Experimental (black) and simulated (red) ESR spectra of the anion radicals of (a) [5,6] and (b) [6,6] benzocycloadducts of Sc₃N@C₈₀. The insets show fragments of the carbon cage denoting the bonds at which the cycloadducts are attached (thick green lines).

ESR spectra of the isomeric anion radicals obtained by reaction of the cycloadducts with cobaltocene. Both compounds exhibit Sc-based hyperfine structure extended over 530 G for the [5,6] adduct and over 670 G for the [6,6] adduct. In spite of the almost identical molecular structures, the hyperfine patterns of the two isomers are remarkably different. The spectrum of the [5,6] benzoadduct exhibits a ⁴⁵Sc coupling pattern corresponding to one nucleus with a 9.1 G splitting and two equivalent nuclei with a 33.3 G coupling and a line width of ca. 1.5 G (Figure 2a). This spectrum is very similar to that of the [5,6] pyrrolidino adduct that was reported recently.²³ All three Sc atoms have considerable spin densities and hence contribute to the complex multiline hyperfine structure (which is additionally complicated by second-order effects). The hyperfine structure for the anion radical of the [6,6] isomer (Figure 2b) is simpler and corresponds to the coupling of the unpaired electron spin to two equivalent Sc nuclei with *a*(⁴⁵Sc) values of 47.9 G. The hfc constant of the third Sc atom is ca. 0.6 G. The value could not be precisely determined because it is smaller than the line width (ca. 1.3 G), but the simulation of the ESR spectrum without the third Sc hyperfine splitting did not provide a good fit to the experimental spectrum. The *g* factors of both radicals (Table 1) are significantly shifted from the free-electron value (*g*_e = 2.0023). Large hfc values and considerable shifts of the *g* factor point to the predominant localization of the spin density on the Sc₃N cluster, similar to what is observed for the anion radical of pristine Sc₃N@C₈₀.^{11,12} Thus, the reductions of the

Table 1. ^{45}Sc Hyperfine Coupling Constants of the Anion Radicals of $\text{Sc}_3\text{N}@\text{C}_{80}$ and Its Derivatives

compd	$N_{\text{C}(\text{sp}^3)}^a$	$a(^{45}\text{Sc})$ (G) ^b	g factor	ref ^c
$\text{Sc}_3\text{N}@\text{C}_{80}$	0	3×55.6	1.9992	11
[5,6] pyrrolidino	2	$9.6, 2 \times 33.4$	1.9972	23
[5,6] benzo				
exptl	2	$9.1, 2 \times 33.3$	1.9982	t.w.
calcd 5/6-I	2	$6.0, 2 \times 15.0$	1.9993	t.w.
calcd 5/6-II	2	$0.3, 2 \times 27.9$	1.9991	t.w.
[6,6] benzo				
exptl	2	$\sim 0.6, 2 \times 47.9$	1.9971	t.w.
calcd 6/6-I	2	$-2.0, 2 \times 39.8$	1.9978	t.w.
$\text{Sc}_3\text{N}@\text{C}_{80}(\text{CF}_3)_2$	2	$2 \times 9.34, 10.7$	1.9958	25
$\text{Sc}_3\text{N}@\text{C}_{80}(\text{CF}_3)_{10}$	10	$\sim 0.6, 11.1, 21.5$	2.0009	43
$\text{Sc}_3\text{N}@\text{C}_{80}(\text{CF}_3)_{12}$	12	$\sim 0.6, 7.4, 8.1$	2.0023	43

^aNumber of $\text{C}(\text{sp}^3)$ atoms. ^bExperimental values, unless noted “calcd” in the first column. ^ct.w. = this work.

benzocycloadducts are endohedral redox processes. However, unlike the nonfunctionalized molecule, both cycloadducts have inhomogeneous spin density distributions among the Sc atoms, as discussed in detail below.

Table 1 compares the ^{45}Sc hfc constants for anion radicals of different $\text{Sc}_3\text{N}@\text{C}_{80}$ derivatives. For all of the studied anion radicals, the hfc constants are smaller than for the anion radical of pristine $\text{Sc}_3\text{N}@\text{C}_{80}$. The smallest $a(^{45}\text{Sc})$ values are found in multiply trifluoromethylated $\text{Sc}_3\text{N}@\text{C}_{80}$ derivatives with 10 and 12 CF_3 groups attached.⁴³ The compounds with only two sp^3 -hybridized carbon atoms in the fullerene cage have very different sets of hfc constants depending on the position of the exohedral group attached to the fullerene cage. In all four derivatives of this kind studied so far, the Sc atoms of the cluster are divided into a pair of equivalent atoms and one Sc atom with different properties. Therefore, cluster rotation is frozen for all of the derivatives, at least on the ESR time scale. The [6,6] adduct exhibits the largest $a(^{45}\text{Sc})$ values, 47.9 G for the two equivalent Sc atoms. For the [5,6] adducts the values are decreased to 33 G, whereas for the $\text{Sc}_3\text{N}@\text{C}_{80}(\text{CF}_3)_2$ bisadduct with two CF_3 groups bonded to a hexagon at the para positions, the smallest hfc values (9.3 G) are observed.²⁵ The opposite trend is revealed for the hfc constant of the third Sc atom: the value increases in going from the [6,6] adduct to the [5,6] adduct to $\text{Sc}_3\text{N}@\text{C}_{80}(\text{CF}_3)_2$. The ESR spectra show that small variations of the π system of the $\text{Sc}_3\text{N}@\text{C}_{80}$ derivative dramatically affect the spin density distribution in the endohedral cluster.

Conformers of $\text{Sc}_3\text{N}@\text{C}_{80}$ Benzoadducts. To probe how exohedral derivatization affects the endohedral cluster of $\text{Sc}_3\text{N}@\text{C}_{80}$ cycloadducts, we performed DFT computations and molecular dynamics simulations. First, we studied how modification of the π system affects the orientation of the Sc_3N cluster. Earlier we reported a detailed study of [5,6]-pyrrolidino- $\text{Sc}_3\text{N}@\text{C}_{80}$,²³ and the results observed for [5,6]-benzo- $\text{Sc}_3\text{N}@\text{C}_{80}$ show that the exohedral group has a weak influence on the energetics of the conformers. The two lowest-energy conformers of the [5,6] benzocycloadducts (5/6-I and 5/6-II; Figure 3a), with relative energies of 0.0 and 3.4 kJ/mol, are similar since the plane of the cluster is perpendicular to the plane of the fused benzene group and two Sc atoms of the cluster are coordinated to the fullerene cage near the $\text{C}(\text{sp}^3)$ atoms. The only difference between the two conformers is a slightly different position of the third Sc atom. Importantly, the

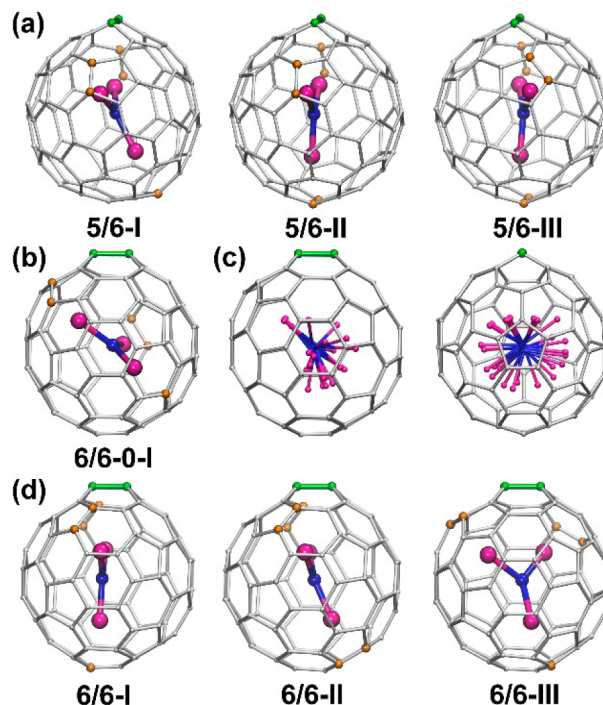


Figure 3. DFT-optimized conformers of the benzocycloadducts of $\text{Sc}_3\text{N}@\text{C}_{80}$: (a) the three lowest-energy conformers of the [5,6] adduct anion; (b) the lowest-energy conformer of the noncharged [6,6] adduct; (c) positions of the Sc_3N cluster in the 10 most stable conformers of the [6,6] adduct (two orientations of the structure are shown); (d) the three lowest-energy conformers of the [6,6] adduct in the anionic state. In all of the structures, the fused benzene moiety has been omitted, and the edge to which the cycle is added is highlighted in green; the Sc-coordinated cage carbon atoms are shown in orange.

orientation of the Sc_3N cluster in conformer 5/6-I corresponds to that reported from the single-crystal X-ray structure of the [5,6] benzocycloadduct.²²

For fused [6,6]-benzo- $\text{Sc}_3\text{N}@\text{C}_{80}$, we generated 52 conformers in which the benzene ring is fused to all nonequivalent 6/6 edges in the lowest-energy C_3 - and C_s -symmetric conformers of $\text{Sc}_3\text{N}@\text{C}_{80}$ and optimized all of the structures at the PBE level. The procedure resulted in 44 nonequivalent conformers for the noncharged cycloadduct whose energies vary within a range of 60 kJ/mol (vs ca. 10 kJ/mol for the conformers of pristine $\text{Sc}_3\text{N}@\text{C}_{80}$). The lowest-energy conformer, 6/6-0-I (Figure 3b), exhibits a position of the Sc_3N cluster similar to that observed for the cluster with the highest population in the experimentally reported X-ray structure.²² However, the distribution of the conformers over the energy range is very dense: e.g., there are 10 conformers of the [6,6] adduct compound with relative energies of less than 10 kJ/mol having very different positions of the cluster (Figure 3c), compared with only two conformers for the [5,6] adduct (Figure 3a).

Addition of one electron to the benzene cycloadducts of $\text{Sc}_3\text{N}@\text{C}_{80}$ has a small effect on the lowest-energy conformers of the [5,6] adduct but results in significant changes for the corresponding [6,6] adduct. For the former, the two lowest-energy conformers (0.0 and 2.0 kJ/mol) are the same as for the neutral state; the third-lowest-energy conformer, 5/6-III, has an energy of 8.6 kJ/mol (Figure 3a). For the anion radical of the [6,6] adduct, the lowest-energy conformers (Figure 3d) are completely different from those of the neutral compound.

Furthermore, the distribution of different conformers over the energy range is not as dense as for the neutral compound. Conformer **6/6-I** is the only structure in the 0–10 kJ/mol range, while the energy of **6/6-II** is 11.5 kJ/mol and that of the third-most-stable conformer, **6/6-III**, is 22.0 kJ/mol.

To summarize, benzyne cycloadditions to [5,6] and [6,6] bonds of $\text{Sc}_3\text{N}@\text{C}_{80}$ result in different dynamic behavior of the endohedral clusters. The [5,6] adduct has a well-defined preferential position of the cluster (**5/6-I**), which is the same for the neutral compound and the anion. On the contrary, for the neutral [6,6] adduct, the cluster exhibits multiple conformations with very close energies, which indicates that the cluster is relatively free to rotate. However, a one-electron reduction of the molecule dramatically changes the situation, resulting in the stabilization of only one particular conformer, **6/6-I**. Importantly, both the **5/6-I** and **6/6-I** conformers have C_s point symmetry, and the symmetry plane is perpendicular to the plane of the cluster. Therefore, two Sc atoms are equivalent, which perfectly agrees with the ESR results.

Spin Density and Hyperfine Coupling Constants. The preferential orientation observed for the Sc_3N cluster in the anion radicals is a prerequisite for the study of the spin density distribution. Figure 4 shows that the unpaired electron in the

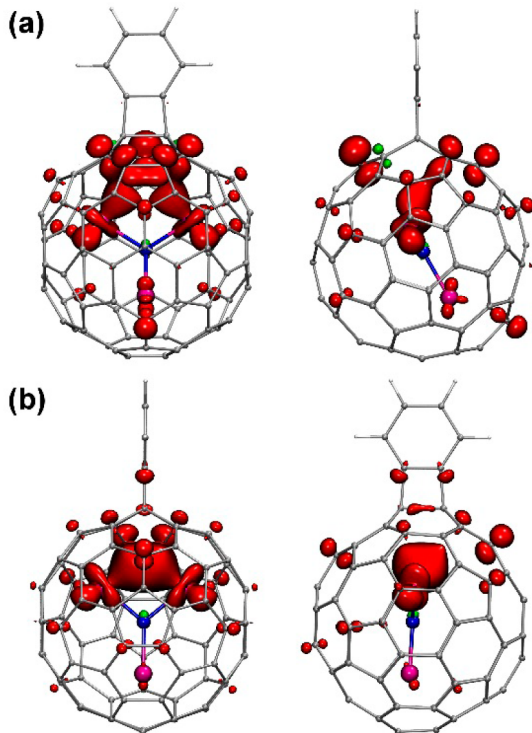


Figure 4. Spatial spin density distributions (PBE functional, isosurface 0.0022) for the lowest-energy conformers of the anion radicals of the benzocycloadducts of $\text{Sc}_3\text{N}@\text{C}_{80}$: (a) [5,6] adduct, conformer **5/6-I**; (b) [6,6] adduct, conformer **6/6-I**. Each structure is shown in two projections.

anion radicals of the **5/6-I** and **6/6-I** conformers is predominantly localized on the two equivalent Sc atoms near the cycloaddition site, whereas the third Sc atom has a very small, almost negligible density. However, in the [5,6] adduct anion radical, the spin density on the carbon cage is more pronounced than for the corresponding [6,6] isomer. The net Mulliken spin population of the Sc atoms for the [6,6] adduct is

0.64, with the two equivalent Sc atoms having populations of 0.32 each and the third Sc atom a population of only 0.02. For the **5/6-I** conformer of the [5,6] adduct, the net spin population is 0.51, where the two equivalent Sc atoms contribute 2×0.22 and the spin population on the third Sc atom is 0.07. The **5/6-II** conformer has a noticeably different spin density distribution: the net Sc population is increased to 0.61, mainly because of the increased populations of the two equivalent Sc atoms (2×0.28). These values can be compared with those of $\text{Sc}_3\text{N}@\text{C}_{80}^-$, in which the net spin population on the three equivalent Sc atoms is 0.80. Thus, cycloaddition results in a significant reduction of the spin density on the cluster, but the degree of this effect depends strongly on the regiochemistry of the addition.

A tentative explanation of the spin density adjustment in the anion radicals of $\text{Sc}_3\text{N}@\text{C}_{80}$ and its derivatives is based on the Pauli repulsion of the surplus electron density on the Sc atom and the endohedral part of the π -electron density of the carbon cage. As discussed in ref 8 and illustrated in Figure 5, the shape

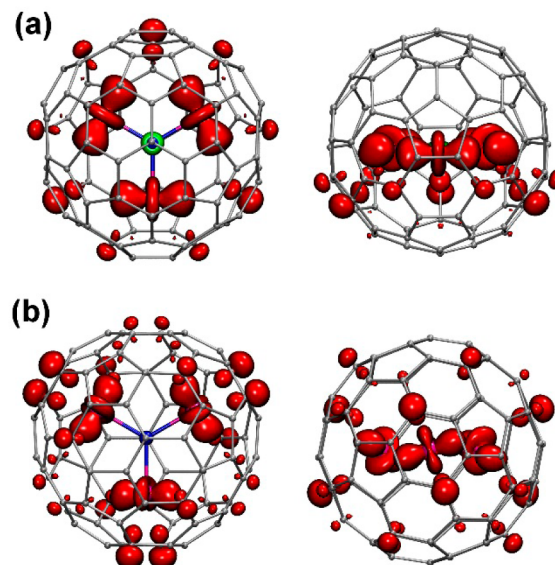


Figure 5. Spatial spin density distributions (PBE functional, isosurface 0.002) in $\text{Sc}_3\text{N}@\text{C}_{80}^-$: (a) C_{3v} conformer; (b) D_3 conformer. Each structure is shown in two projections with the plane of the Sc_3N cluster either (left) parallel or (right) perpendicular to the paper.

of the spin density lobes localized on Sc atoms in $\text{Sc}_3\text{N}@\text{C}_{80}$ anion depends strongly on the position of the cluster with respect to the cage and on the hapticity of the metal-cage coordination sites. In the lowest-energy C_{3v} conformer with [5,6]-CC bonds η^2 -coordinated by Sc atoms (Figure 5a), the shape resembles that of the d_{z^2} orbital whose z axis is parallel to the [5,6] edge. The main lobes of the Sc-localized spin density point to the centers of hexagons, where the electron density is minimal. Besides, the largest overlap with the cage atom is for the carbon atoms at triple-hexagon junctions (THJs) [such atoms are known to have the least negative charges according to quantum theory of atoms in molecules (QTAIM) analysis⁴⁴]. We propose that such a configuration minimizes the repulsion and enables maximized spin populations for the Sc atoms. When Sc atoms are coordinated to the centers of hexagons in an η^6 manner, as in the D_3 -symmetric conformer shown in Figure 5b, the shape of the Sc-localized spin density has a more complex shape and resembles a combination of a d_{z^2}

orbital and a d_{xz} orbital (whose plane is parallel to the cage surface). It appears that in such a configuration the Coulomb repulsion is stronger, which leads to a larger overlap with the cage and reduces the spin population of Sc atoms (0.17 in the D_3 conformer vs 0.27 in the C_{3v} conformer).

In the two conformers of $\text{Sc}_3\text{N}@\text{C}_{80}$ discussed above, threefold symmetry is imposed, and all of the Sc atoms are equivalent. When less symmetric positions of the Sc_3N cluster are considered, the spin density can be unequally redistributed among the Sc atoms so that the atoms with low density repulsion have enhanced spin populations. This is exactly what happens in the anion radicals of $\text{Sc}_3\text{N}@\text{C}_{80}$ cycloadducts. Furthermore, cycloaddition makes a “void” in the carbon π density under the functionalized CC bond, which opens the possibility for a further reduction of the repulsive interactions in anions via localization of the surplus electron density near this void. As can be seen in Figure 4, the largest spin density lobes in both the [5,6] and [6,6] isomers of the benzoadduct are located exactly below the functionalized 5/6 and 6/6 edges, respectively.

The DFT-computed hfc constants for the 5/6-I, 5/6-II, and 6/6-I conformers are listed in Table 1. The computed values are systematically underestimated, but the overall qualitative agreement is rather good, especially for the [6,6] adduct (compare the experimental value of 47.9 G to the calculated constant of 39.8 G). For the [5,6] adduct, slight variations of the cluster position in the two almost isoenergetic conformers doubles the hfc value for the two Sc atoms from 15.0 G in 5/6-I to 27.9 G in 5/6-II. This shows that the $a(^{45}\text{Sc})$ values are very sensitive to the cluster orientation, as already reported in our earlier studies of the $\text{Sc}_3\text{N}@\text{C}_{80}^-$ and [5,6]-pyrrolidino- $\text{Sc}_3\text{N}@\text{C}_{80}^-$ anions.^{8,23}

Molecular Dynamics Simulations. When several conformers with low barriers of interconversion are available, the use of a static approach to analyze the spin density and coupling constants may not necessarily be reliable.^{13,24,45} To clarify whether dynamic effects are critical for the interpretation of the results observed for the anion radicals of the $\text{Sc}_3\text{N}@\text{C}_{80}$ benzocycloadducts, we performed DFT-based molecular dynamics simulations at the PBE/DZVP level. Figure 6a,b shows trajectories obtained after observation of the anion over 12 ps starting from the lowest-energy conformers 5/6-I and 6/6-I, respectively. In agreement with the static DFT calculations, the [5,6] adduct exhibits a more pronounced displacements of the Sc atoms (Figure 6a) than the [6,6] adduct, in which the cluster remains almost fixed during the whole trajectory (Figure 6b). In line with this dynamic behavior, the oscillations of the spin populations along the trajectory are much more pronounced for the [5,6] adduct (Figure 6c) than for the [6,6] adduct (Figure 6d). Nevertheless, in both cases the net spin populations vary over a rather broad range, showing that dynamic effects are not totally negligible. However, when averaged over the whole trajectory, the values obtained are very close to the results from the static calculations for the spin populations of the Sc atoms. The ^{45}Sc hfc constants integrated over the MD trajectory are 3.5 and 2×25.5 G for the [5,6] adduct and -1.1 and 2×31.7 G for the [6,6] adduct.

CONCLUSIONS

In this work we have performed ESR spectroscopic and computational studies of the anion radicals of the two isomeric benzoadducts of $\text{Sc}_3\text{N}@\text{C}_{80}$ with [5,6] and [6,6] addition patterns. In comparison to the freely moving Sc_3N cluster in

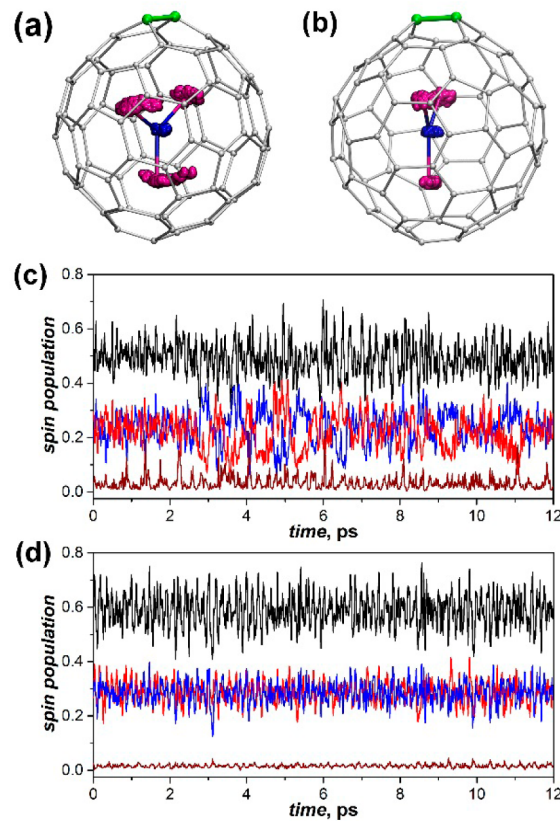


Figure 6. Molecular dynamics simulations (300 K) for the anion radicals of the benzocycloadducts of $\text{Sc}_3\text{N}@\text{C}_{80}$. (a, b) 12 ps trajectories of the (a) [5,6] and (b) [6,6] adducts. Displacements of carbon atoms are not shown, and the cycloaddition site is highlighted in green. (c, d) Instantaneous spin populations of the Sc atoms computed along the MD trajectories of the (c) [5,6] and (d) [6,6] adducts. In each panel, the black line denotes the net Sc population, the red and blue lines represent the two equivalent Sc atoms, and the brown line denotes the third Sc atom.

pristine $\text{Sc}_3\text{N}@\text{C}_{80}^-$, all of the derivatives exhibit reasonably fixed cluster positions, inhomogeneous spin density distributions, and large variations in the hfc values within the cluster. It was also found that exohedral derivatization significantly reduces the net spin population on the Sc atoms in the cluster, and interestingly, the effect is markedly dependent on the regiochemistry of the adduct site on the fullerene cage. The high structural specificity of the ESR spectroscopic data makes ESR spectroscopy a valuable tool for the study of cluster structure and dynamics in EMF compounds and their derivatives.

ASSOCIATED CONTENT

S Supporting Information

DFT-optimized Cartesian coordinates and energies of the conformers shown in Figure 3. This material is available free of charge via the Internet at <http://pubs.acs.org>.

AUTHOR INFORMATION

Corresponding Authors

a.popov@ifw-dresden.de
echegey@utep.edu

Present Address

^{II}F.-F.L.: Department of Chemistry, George Washington University, Washington, DC 20052, USA.

Notes

The authors declare no competing financial interest.

ACKNOWLEDGMENTS

The authors are thankful to Ulrike Nitzsche and Marco Rosenkranz (both at IFW Dresden) for assistance with local computational resources and ESR measurements. The Research Computing Center of Moscow State University⁴⁶ and The Center for Information Services and High Performance Computing of Technical University of Dresden are acknowledged for computing time. Financial support by the DFG (Project PO 1602/1–1 to A.A.P.), the National Science Foundation (Grant CHE-1408865 to L.E.), and the Robert A.Welch Foundation (endowed chair to L.E., Grant AH-0033) is highly appreciated. L.E. also thanks the NSF (Grant CHE-1228325 from the MRI Program) for the purchase of an ESR spectrometer.

REFERENCES

- (1) Popov, A. A.; Yang, S.; Dunsch, L. *Chem. Rev.* **2013**, *113*, 5989.
- (2) Chaur, M. N.; Melin, F.; Ortiz, A. L.; Echegoyen, L. *Angew. Chem., Int. Ed.* **2009**, *48*, 7514.
- (3) Lu, X.; Feng, L.; Akasaka, T.; Nagase, S. *Chem. Soc. Rev.* **2012**, *41*, 7723.
- (4) Rodriguez-Fortea, A.; Balch, A. L.; Poblet, J. M. *Chem. Soc. Rev.* **2011**, *40*, 3551.
- (5) Wang, T.; Wang, C. *Acc. Chem. Res.* **2014**, *47*, 450.
- (6) Popov, A. A.; Dunsch, L. *J. Phys. Chem. Lett.* **2011**, *2*, 786.
- (7) Zhang, Y.; Popov, A. A. *Organometallics* **2014**, DOI: 10.1021/om5000387.
- (8) Popov, A. A.; Dunsch, L. *J. Am. Chem. Soc.* **2008**, *130*, 17726.
- (9) Valencia, R.; Rodriguez-Fortea, A.; Clotet, A.; de Graaf, C.; Chaur, M. N.; Echegoyen, L.; Poblet, J. M. *Chem.—Eur. J.* **2009**, *15*, 10997.
- (10) Iiduka, Y.; Ikenaga, O.; Sakuraba, A.; Wakahara, T.; Tsuchiya, T.; Maeda, Y.; Nakahodo, T.; Akasaka, T.; Kako, M.; Mizorogi, N.; Nagase, S. *J. Am. Chem. Soc.* **2005**, *127*, 9956.
- (11) Jakes, P.; Dinse, K. P. *J. Am. Chem. Soc.* **2001**, *123*, 8854.
- (12) Elliott, B.; Yu, L.; Echegoyen, L. *J. Am. Chem. Soc.* **2005**, *127*, 10885.
- (13) Popov, A. A.; Chen, C.; Yang, S.; Lipp, F.; Dunsch, L. *ACS Nano* **2010**, *4*, 4857.
- (14) Stevenson, S.; Rice, G.; Glass, T.; Harich, K.; Cromer, F.; Jordan, M. R.; Craft, J.; Hadju, E.; Bible, R.; Olmstead, M. M.; Maitra, K.; Fisher, A. J.; Balch, A. L.; Dorn, H. C. *Nature* **1999**, *401*, 55.
- (15) Heine, T.; Vietze, K.; Seifert, G. *Magn. Reson. Chem.* **2004**, *42*, S199.
- (16) Cardona, C. M.; Kitaygorodskiy, A.; Ortiz, A.; Herranz, M. A.; Echegoyen, L. *J. Org. Chem.* **2005**, *70*, 5092.
- (17) Cai, T.; Slednick, C.; Xu, L.; Harich, K.; Glass, T. E.; Chancellor, C.; Fettinger, J. C.; Olmstead, M. M.; Balch, A. L.; Gibson, H. W.; Dorn, H. C. *J. Am. Chem. Soc.* **2006**, *128*, 6486.
- (18) Iezzi, E. B.; Duchamp, J. C.; Harich, K.; Glass, T. E.; Lee, H. M.; Olmstead, M. M.; Balch, A. L.; Dorn, H. C. *J. Am. Chem. Soc.* **2002**, *124*, 524.
- (19) Rodriguez-Fortea, A.; Campanera, J. M.; Cardona, C. M.; Echegoyen, L.; Poblet, J. M. *Angew. Chem., Int. Ed.* **2006**, *45*, 8176.
- (20) Aroua, S.; Yamakoshi, Y. *J. Am. Chem. Soc.* **2012**, *134*, 20242.
- (21) Garcia-Borràs, M.; Osuna, S.; Luis, J. M.; Swart, M.; Solà, M. *Chem.—Eur. J.* **2013**, *19*, 14931.
- (22) Li, F.-F.; Pinzon, J. R.; Mercado, B. Q.; Olmstead, M. M.; Balch, A. L.; Echegoyen, L. *J. Am. Chem. Soc.* **2011**, *133*, 1563.
- (23) Elliott, B.; Pykhova, A. D.; Rivera, J.; Cardona, C. M.; Dunsch, L.; Popov, A. A.; Echegoyen, L. *J. Phys. Chem. C* **2013**, *117*, 2344.
- (24) Popov, A. A.; Dunsch, L. *Phys. Chem. Chem. Phys.* **2011**, *13*, 8977.
- (25) Popov, A. A.; Shustova, N. B.; Svitova, A. L.; Mackey, M. A.; Coumbe, C. E.; Phillips, J. P.; Stevenson, S.; Strauss, S. H.; Boltalina, O. V.; Dunsch, L. *Chem.—Eur. J.* **2010**, *16*, 4721.
- (26) Garcia-Borràs, M.; Romero-Rivera, A.; Osuna, S.; Luis, J. M.; Swart, M.; Solà, M. *J. Chem. Theory Comput.* **2012**, *8*, 1671.
- (27) Stoll, S.; Schweiger, A. *J. Magn. Reson.* **2006**, *178*, 42.
- (28) Perdew, J. P.; Burke, K.; Ernzerhof, M. *Phys. Rev. Lett.* **1996**, *77*, 3865.
- (29) Laikov, D. N.; Ustynuk, Y. A. *Russ. Chem. Bull.* **2005**, *54*, 820.
- (30) Laikov, D. N. *Chem. Phys. Lett.* **2005**, *416*, 116.
- (31) Laikov, D. N. *Chem. Phys. Lett.* **1997**, *281*, 151.
- (32) Neese, F. *Wiley Interdiscip. Rev.: Comput. Mol. Sci.* **2012**, *2*, 73.
- (33) Neese, F. Institute for Physical and Theoretical Chemistry: Bonn, Germany, 2010.
- (34) Schäfer, A.; Horn, H.; Ahlrichs, R. *J. Chem. Phys.* **1992**, *97*, 2571.
- (35) Weigend, F.; Ahlrichs, R. *Phys. Chem. Chem. Phys.* **2005**, *7*, 3297.
- (36) Neese, F. *Inorg. Chim. Acta* **2002**, *337*, 181.
- (37) VandeVondele, J.; Krack, M.; Mohamed, F.; Parrinello, M.; Chassaing, T.; Hutter, J. *Comput. Phys. Commun.* **2005**, *167*, 103.
- (38) The CP2K developers group, 2010.
- (39) Lippert, G.; Hutter, J.; Parrinello, M. *Theor. Chem. Acc.* **1993**, *103*, 124.
- (40) Goedecker, S.; Teter, M.; Hutter, J. *Phys. Rev. B* **1996**, *54*, 1703.
- (41) Humphrey, W.; Dalke, A.; Schulten, K. *J. Mol. Graphics* **1996**, *14*, 33.
- (42) Connelly, N. G.; Geiger, W. E. *Chem. Rev.* **1996**, *96*, 877.
- (43) Shustova, N. B.; Peryshkov, D. V.; Kuvychko, I. V.; Chen, Y.-S.; Mackey, M. A.; Coumbe, C. E.; Heaps, D. T.; Confait, B. S.; Heine, T.; Phillips, J. P.; Stevenson, S.; Dunsch, L.; Popov, A. A.; Strauss, S. H.; Boltalina, O. V. *J. Am. Chem. Soc.* **2011**, *133*, 2672.
- (44) Popov, A. A.; Dunsch, L. *Chem.—Eur. J.* **2009**, *15*, 9707.
- (45) Popov, A. A.; Chen, N.; Pinzon, J. R.; Stevenson, S.; Echegoyen, L. A.; Dunsch, L. *J. Am. Chem. Soc.* **2012**, *134*, 19607.
- (46) Voevodin, V. V.; Zhumatiy, S. A.; Sobolev, S. I.; Antonov, A. S.; Bryzgalov, P. A.; Nikitenko, D. A.; Stefanov, K. S.; Voevodin, V. V. Practice of “Lomonosov” Supercomputer. *Open Syst. J.* [Online] **2012** (No. 7). <http://www.osp.ru/os/2012/07/13017641/> (accessed July 25, 2014).